

Dynamo

Dynamic Spatio-Temporal Modulation
of Light by Phononic Architectures.



**Funded by
the European Union**

European
Innovation
Council



D5.1 Experimental setup

Date: 28 April 2023

D.5.1: Experimental set up

WP5. T.5.1: Application development

Author(s) and ORCID(s) ID: Daniel Torrent (0000-0001-7092-7360); Jesús Lancis (0000-0002-7336-6930), Enrique Tajahuerce (0000-0003-1655-4393) Agustín Mihi (0000-0003-3821-7881), Ana Conde-Rubio (0000-0001-5739-2189), Fernando Soldevila (0000-0002-7776-1276) and, Olga Boyko.

1. Version History

Version	Date	Beneficiary	Author
V1.1	27/04/2023	UJI	Daniel Torrent
	Date	Beneficiary	Reviewed by
V1.2	28/04/2023	CSIC, CNRS	Agustín Mihi, Olga Boyko, Fernando Soldevila
	Date	Beneficiary	Approved by
V1.3	28/04/2023	UJI	Daniel Torrent

Dynamo High frequency characterization set-up

Universitat Jaume I

Contact Daniel Torrent, Coordinator of the Dynamo project

Email dtorrent@uji.es

2023 Dynamo

Disclaimer:

“Funded by the European Union. Views and opinions expressed are however those of the author(s) only and do not necessarily reflect those of the European Union or European Innovation Council and SMEs Executive Agency (EISMEA). Neither the European Union nor European Innovation Council and SMEs Executive Agency (EISMEA) can be held responsible for them”.

2. Technical References

Project Number	101046489
Project Acronym	Dynamo
Project Title	Dynamic Spatio-Temporal Modulation of Light by Phononic Architectures
Granting Authority	European Innovation Council and SMEs Executive Agency
Call	HORIZON-EIC-2021-PATHFINDEROPEN-01
Topic	HORIZON-EIC-2021-PATHFINDEROPEN-01-01
Type of the Action	HORIZON EIC Grants
Duration	1 March 2022 - 28 February 2026 (48 months)
Entry into force of the Grant	1 March 2022
Project Coordinator	Daniel Torrent Martí

Deliverable No.	D5.1 Experimental set up
Work Package	WP5 – Application development
Task	T5.1 Development and testing of the fundamental experimental set up
Dissemination level	PU - Public
Type of license	CC-BY
Lead beneficiary	Universitat Jaume I
PIC of the Lead beneficiary	999997930
Contributing beneficiaries	- Agencia Estatal Consejo Superior de Investigaciones Científicas (CSIC) - Centre National de la Recherche Scientifique (CNRS)
PIC of Contributing beneficiaries	- CSIC: 999991722 - CNRS: 999997930
Due date of deliverable	28/02/2023
Actual submission date	28/04/2023

3. Table of contents

1. Version History	2
2. Technical References	3
3. Table of contents	4
4. Introduction	5
4.1. Executive Summary	5
4.2. Relation to Other Project Documents	5
4.3. Abbreviation List	5
4.4. Reference Documents	6
5. Experimental setup for picosecond ultrasonics	6
5.1. The Interferometer	8
5.2. Opto-acoustic modulator	10
5.3. Second harmonic generator	10
5.4. The delay line	10
5.5. The imaging system	11
5.6. The synchronous detection	12
6. Future improvements	14
7. Conclusion	15

4. Introduction

4.1. Executive Summary

The objective of Work Package 5 (WP5) is to develop imaging applications for the samples designed by our project partners AGH, IC, and UJI, which were fabricated by CSIC and characterized by CNRS. This work package represents the final step in the process described in this project. To develop these applications, we need to excite the phononic modes previously characterized at CNRS. Due to the complex nature of experiments in this domain, we cannot expect the spatial distributions of the field to be identical to those measured by CNRS, although the frequencies at which these are excited will be identical or very close. For a proper development of applications, it is desirable then that the experiments be as similar as possible. For this reason we proposed to implement the setup with the same elements, especially the laser source.

Therefore, the first task of WP5 was to replicate the picosecond ultrasonic setup of CNRS so that we can later develop applications based on the optimal phononic architectures. Despite some delays in acquiring the necessary equipment, we have finally completed the setup, and it is working correctly. We can now excite acoustic waves in the range of a tenth of a GHz and accurately resolve these waves over time.

In this document, we will explain the different components of the setup, including relevant parameters of the electronic equipment, and provide a list of immediate improvements to optimize the measurements, particularly regarding the spatial scanning of the acoustic fields. However, it's important to note that, like any homemade experimental setup, technical improvements will continuously be implemented throughout the project's duration.

4.2. Relation to Other Project Documents

The present document is related with the Deliverable 4.2. High frequency characterisation set-up (CNRS, SEN, M13).

4.3. Abbreviation List

PBS: Polarizing beam splitter
M: Mirror
MO: Microscope objective
HW: Half-wave plate
QW: Quarter-wave plate
PD: Photodiode
DM: Dichroic mirror
PS: Power splitter
AOM: Acousto-optic modulator
SHG: Second harmonic generator
Pb: Probe
Pm: Pump

4.4. Reference Documents

The current version of the setup was implemented according to the schematics of the following reference:

Tachizaki, T., Muroya, T., Matsuda, O., Sugawara, Y., Hurley, D. H., & Wright, O. B. (2006). Scanning ultrafast Sagnac interferometry for imaging two-dimensional surface wave propagation. *Review of Scientific Instruments*, 77(4), 043713.

5. Experimental setup for picosecond ultrasonics

Figure 1 shows the schematic of the experimental setup for the excitation and detection of acoustic waves around the GHz, and figure 2 shows a picture of some relevant elements. In this version of the setup, three laser pulses hit a 50nm sample of chromium deposited on a glass substrate. The three pulses correspond, in order of arrival, to "probe 1" or Pb1, to "pump" or Pm and to "probe 2" or Pb2.

The three pulses are generated by the successive division of the 800nm laser beam emitted by the laser source (model Chameleon Ultra II of Coherent). As we can see in figure 1, this beam is attenuated by the power splitter PS, since of the 4W of power that it emits, we only use 1W. With the half-wave plate HW1 we control the amount of energy that goes to the "probe" beam and to the "pump", the former indicated with a continuous line in the figure and the latter by the dotted line. Almost all the energy (around 90%) goes through the "pump" line, which with two mirrors is directed to the acousto-optic modulator AOM and then directed again towards the second harmonic crystal SHG. The modulator generates a 1.6 MHz envelope in the laser pulse train, and finally it is doubled in frequency to excite the sample by means of the dichroic mirror DM and the microscope objective (MO). In the current version of the setup, we use a 40x magnification objective, which would be replaced by a higher magnification one (100x) in the final version so that we can excite SAWs in the range of several GHz.

The electric field from the "probe" is again rotated with the half-wave plate (HW2) so that it goes through the polarizing beam splitter (PBS2) and goes through the 2 ns delay line. When leaving the delay line, the beam goes through a quarter-wave plate (QW1), it is reflected in mirror M1 and passes again through QW1 and the delay line, so that its polarization has now been rotated 90 degrees and is reflected by PBS2 to enter the Sagnac-type interferometer. This double passage through the delay line can provide us with a delay with respect to the "pump" of up to 4 ns.

The probe then reaches the half-wave plate HW3, with which we choose the intensity that we want to send in each direction of the polarizing beam splitter PBS3 (the non-polarizing beam splitter NPBS does not play any role in this first path). It is therefore PBS3 the element that divides the "probe" into Pb1 and Pb2. The first one is reflected, it passes through QW4 and through MO to focus on the sample, then it returns through MO and passes through QW4 so that its polarization has been rotated and now it goes through PBS3, bounces off M2 and M3, goes through PBS3 again to reflect on NPBS and goes to PBS4, traversing it to enter the first channel of the balanced photodiode. When passing through HW3 and NPBS, the Pb2 beam follows the same path but in the opposite direction. That is, it crosses PBS3 and is reflected in M3 and M2, passing through PBS3 again and through QW4, MO, the sample and again MO and QW4, thereby rotating its polarization so that it is now reflected by PBS3, but also by NPBS and PBS4, thus

reaching the second channel of the photodiode. The difference between the two intensities is amplified and sent to the lock-in amplifier, which will detect any component at 1.6. MHz that exists in said difference. This component can only be due to the Pm that arrives after Pb1, so Pb2 is measuring the effect of Pm on the sample. By controlling the delay line, we can determine at what instant after the arrival of Pm we measure the difference between the reflectance at rest and the reflectance from the excitation.

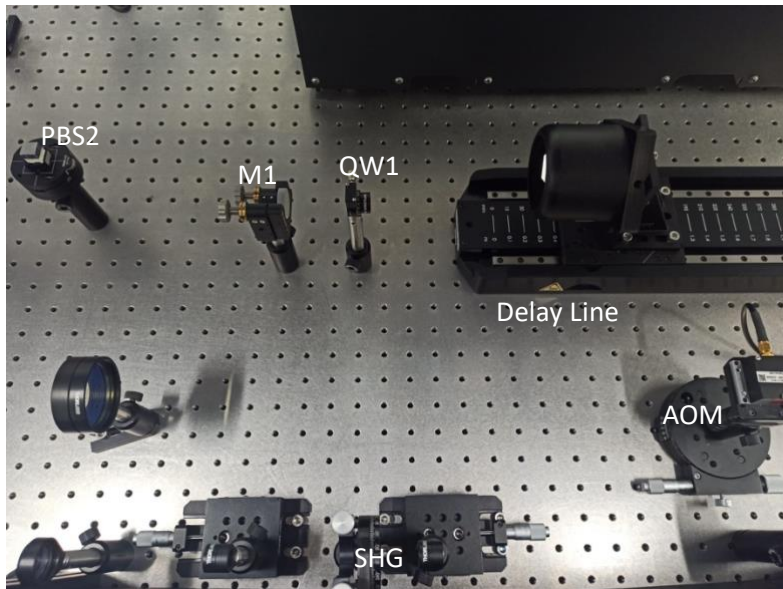


Figure 1. Picture of one area of the setup with the AOM, the SHG and the delay line.

Since Pb1 and Pb2 have a delay of approximately 1 ns, if the phenomenon we want to study lasts less than that time, we ensure a difference with respect to rest. For when this is not the case, we have two alternatives. The first one is to increase the relative delay between Pb1 and Pb2, the second one is to decrease it until the measurement we have is proportional to the time derivative of the reflectance.

The setup has been tested with a sample consisting of a thin layer of chromium (50nm thickness) deposited on a glass substrate. Figure 4 shows the preliminary results that we have obtained with this setup, where we can see the heating-cooling curve of the sample due to the "pump". The horizontal axis represents time, measured in ps (picoseconds), while the vertical axis shows the reflectance variation of the sample

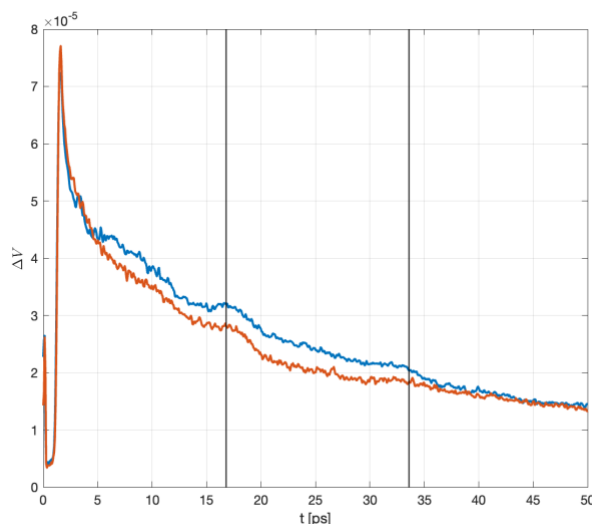


Figure 3 Preliminary experimental data, corresponding to the heating-cooling of a 50nm thin film of chromium over a glass substrate.

measured by the lock-in, which detects a signal that varies from 0 to 80 mV rapidly and then decays exponentially. The two traces correspond to two measurements on the same point of the sample. This reflectance variation is directly proportional to the variation of the surface's temperature of the sample. The two vertical lines at $t=16.8$ ps and $t=2 \times 16.8$ ps show the times that an acoustic pulse travels through the 50 nm thickness of the sample, bounce off the glass, and return to the surface, causing a change in reflectance due to the

photoelastic effect. We see that, indeed, there is a small variation of the reflectance due

to the first pulse, and we can also guess a smaller variation in the second pulse, which has bounced off the surface to return to the glass and back to the first surface.

The setup is therefore working, and we can excite and detect acoustic waves on thin layers. Within the next months we will refine the setup with the improvements explained at the end of the report, after the explanation of the different parts of the system.

5.1. The Interferometer

Figure 4 shows the two possible configurations for the interferometer as described before. The Michelson-like interferometer allows, in principle, for a simpler alignment; however, it requires the use of three quarter-wave plates and if the quality of the polarization state is not good, some spurious reflections appear as a background in the measured signal. It is easy to follow the path of the two probe beams, since one goes directly to the sample after PBS and then goes back to the photodiode after passing through the two mirrors and NPBS, while the other beam makes the same path but in the reverse direction.

As we explained before, we used the Sagnac-like with the two-mirror configuration shown in figure 4, although placing M1 and M2 at 45° and adding an additional mirror would allow us to tune the time delay between the two probe beams. While this additional control complicates alignment, it makes possible to change the delay time between the two probe beams from nearly 100 ps to several nanoseconds, thus allowing to change from the measurement of the time-dependent reflectance to its derivative. We keep this as a possible improvement for future versions of the setup, although for the next months we will keep the configuration with only two mirrors.

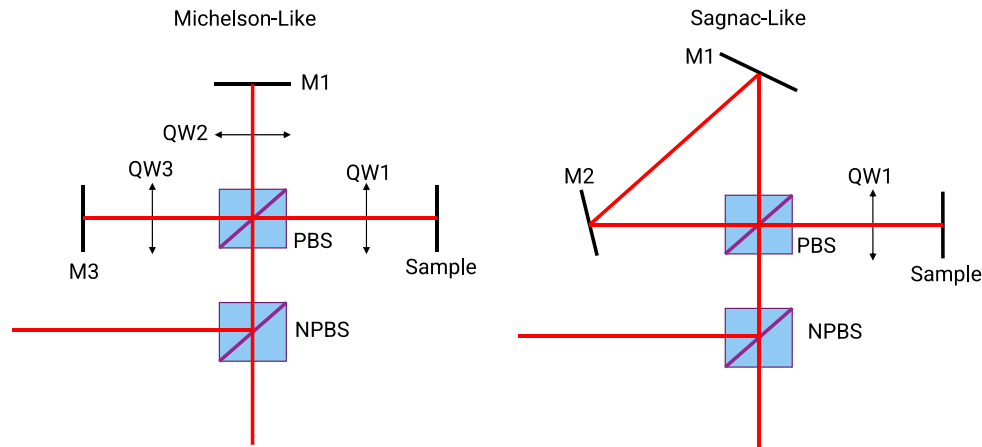


Figure 4 Schematics of the two interferometers tested for the setup

Extracting information from the measurement of the difference between the two probe intensities is not an obvious task in a picosecond ultrasonics experiment, where the excitation of the sample changes both the phase and modulus of its reflectance. Thus, after the NPBS in both types of interferometers the state of the electric field is such that the two probe beams have orthogonal polarizations. We can write this polarization as

$$E = \begin{pmatrix} R_0(1 + \rho_1)e^{i\phi_1} \\ R_0(1 + \rho_2)e^{i\phi_2} \end{pmatrix}$$

where ρ_i is the (small) variation of the reflectance of the sample due to the pump and ϕ_i is its phase, which will be mainly due to the vertical displacement of the surface of the sample. We will assume that probe 1 arrives before probe 2. Both pulses arrive very close in time and after the pump (although in our current version of the setup this is not the case, probe 1 arrives before the pump so $\rho_1 = 0$ and $\phi_1 = 0$, but this case will be discussed at the end of the explanation below).



Figure 5 Picture of the Sagnac-Like interferometer

If before entering the balanced photodiode we introduce a quarter wave plate with its fast axis oriented at 45° , such that its Jones matrix is as follows:

$$M_{\lambda/4} = \begin{pmatrix} 1 + i & 1 - i \\ 1 - i & 1 + i \end{pmatrix}$$

the electric field before the plate is given by

$$E_1 = R_0(1 + \rho_1)e^{i\phi_1} \approx R_0(1 + \rho_1 + i\phi_1)$$

$$E_2 = R_0(1 + \rho_2)e^{i\phi_2} \approx R_0(1 + \rho_2 + i\phi_2)$$

and after the plate will be

$$\begin{aligned} \frac{E'_1}{R_0} &= (1 + i)(1 + \rho_1 + i\phi_1) + (1 - i)(1 + \rho_2 + i\phi_2) \\ &= 2 + \rho_1 + \rho_2 - \phi_1 + \phi_2 + i(\rho_1 - \rho_2 + \phi_1 + \phi_2) \end{aligned}$$

$$\begin{aligned} \frac{E'_2}{R_0} &= (1 - i)(1 + \rho_1 + i\phi_1) + (1 + i)(1 + \rho_2 + i\phi_2) \\ &= 2 + \rho_1 + \rho_2 + \phi_1 - \phi_2 + i(\rho_2 - \rho_1 + \phi_1 + \phi_2) \end{aligned}$$

If we take the modulus of the above expressions, we will have the intensities arriving at each photodiode, thus we have

$$I_1 \approx \rho_1 + \rho_2 - \phi_1 + \phi_2$$

$$I_2 \approx \rho_1 + \rho_2 + \phi_1 - \phi_2$$

And taking their difference (which is the signal sent to the lock-in amplifier)

$$I_2 - I_1 \approx \Delta t \frac{\partial \phi}{\partial t}$$

Similarly, if the quarter wave plate is rotated, it is easy to see that the measurement we get is

$$M_{\lambda/4} = \begin{pmatrix} i & 0 \\ 0 & 1 \end{pmatrix} \rightarrow I_2 - I_1 \approx \Delta t \frac{\partial \rho}{\partial t}$$

Therefore, by rotating the quarter wave plate we can swap between a measurement of the derivative of the phase or a measurement of the modulus of the reflectance. If the time difference between the two probes is very large and probe 1 arrives before the pump (so that $\rho_1 = 0$ and $\phi_1 = 0$), what we detect is directly the phase and modulus of the reflectance. In the current version of the setup, we don't have yet the quarter wave plate, so our measurement is equivalent to the last situation in which we measure the relative variations of the modulus of the reflectance. However it seems that, for now, this is enough to detect even surface acoustic waves by means of the photoelastic effect.

5.2. Opto-acoustic modulator

The opto-acoustic modulator (AA Opto-electronic MT200-A0,5-800) modulates the pump beam at 1.6 MHz prior to the second harmonic conversion. This modulation will be transferred to the reflectance of the sample by means of a thermoelastic coupling. The OAM acts as a time-dependent grating generating It generates many orders (0, +1, +2, etc.). The OAM acts as a time-dependent grating, whose diffraction orders (other than the zero order) oscillate at the driver frequency. For an optimal performance, where most of the energy is deposited into a single diffraction order (the first one), the beam must enter the OAM with the right orientation. We control this by placing the OAM on a three-axis optomechanical mount, which allows for fine adjustment. We have arrived to an efficiency of the diffracted beam of more than 40%.

Another important element to enhance the diffraction efficiency is the size of the beam entering into the OAM, to optimize this point a long focal length lens (50 cm) is placed before the OAM to focus it on the crystal and an identical lens after it to collimate again the beam.

5.3. Second harmonic generator

The second harmonic generator consists in a nonlinear crystal (Eksma Optics BBO-603H) mounted on a positioning mount with three degrees of freedom (Eksma Optics Reference 840-0199). The angle of incidence of the beam and its polarization is important for an efficient conversion, so these degrees of freedom are required. Also, the energy density arriving to the crystal is an important parameter for the conversion, for this reason we put a convergent lens of 20 mm of focal length (not shown in the schematics of figure 1) before the crystal and after it to recover collimation. An 800 nm narrowband filter is placed after the second lens to block the residual light coming from the crystal. After fine tuning of the different parameters (lenses, polarization, and incident angle) we got a power of nearly 10mW at a wavelength of 400 nm, enough for the generation of SAWs.

5.4. The delay line

The delay line is an important part of the picosecond ultrasonics setup. The short pulses generated by the pump laser cannot be generally monitored in common oscilloscopes, besides the fact that the weak signal generated by the change of the reflectance needs to be detected by a lock-in amplifier, as explained before. The delay line allows therefore

to change the time at which the probe beams arrive to the sample to interrogate its status, and this time can be selected with a precision of about 0.03 ps.

The repetition rate of the laser is of 80MHz, so that the experiment performed is a stroboscopic experiment that repeats every 12.5ns. In principle, the delay line should allow us to explore the full repetition period, but at this moment we can monitor only one third of this time (4ns). The reason behind this is that the high precision linear stage we have acquired (Newport DL325) is only 325cm long, which gives a delay of about 2ns. Since in the configuration we have proposed the probe beam passes through the delay line two times, the total delay is of 4ns.

For the current phenomena this is enough, since the pulses we excite last less than four nanoseconds, the only challenge is to be able to locate the exact position at which the experiment starts within the 12.5 ns window. Thus, it is important that we be able to configure the system such that in the window of 4ns the pump and probe arrives at the same time. This can be done by roughly measuring the path followed by the two beams in the optical table to later fine tuning the distances. To be sure that this is happening, a preliminary calibration of the setup is done by putting a fast photodiode just before the microscope objective and checking that, by moving the delay line, we can get at the same time both the pump and probe beams.

Another important configuration of the setup is the right alignment of the delay line. We must guarantee that when the delay line travels there is no movement of the focusing point of the probe beams in the sample. This alignment can be done in several steps, and it requires some practice. To minimize mistakes, we used a beam profiler just before the sample after fine alignment of the beam by sending it to a faraway point in the lab. Always that it has been possible we have aligned the beams with the lattice of holes of the table and all the beams are at 12 cm over the table.

5.5. The imaging system

The imaging system is not drawn in figure 1 for simplicity, but as can be seen from the figure it consists in simple glass-lens-camera system that allow us to make an image of the sample in the camera. In our setup the lens is a convergent lens of 6mm of focal length, although we have tried several options. The thin glass is a microscope sample

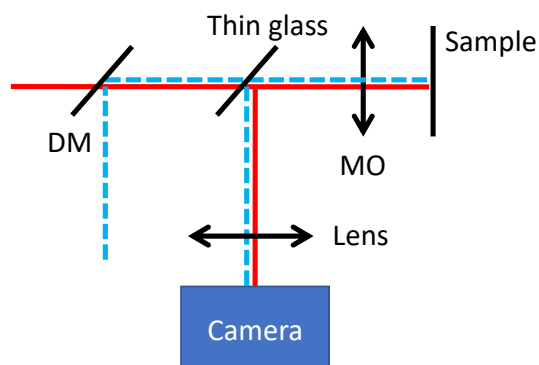


Figure 6 Schematics of the imaging system to visualize the position of the pump and probe beams on the sample

holder of less than 100 μm of thickness, so that its effect on the beam path is negligible. The illumination system to see the possible damage of the sample as well as the exact position on the nanostructure is not yet implemented, and there is room for improvement on the imaging system itself. Although for elementary pump&probe measurements this is enough, since our aim is to develop imaging applications, we need to improve this part of the setup within the next months. All the elements in this part of the setup have several optomechanical

components that allow us for an accurate position and alignment of the optics of the

system. Although we can add or remove some elements in the future, at this time we have the following elements:

1. The DM is attached on a two-angle tilt mount.
2. The sample is on a two-angle tilt mount and the full structure is mounted on a three-axis translation stage.
3. The microscope objective is on a two-angle tilt mount, but we found this redundant in the setup. However, we will add a horizontal-vertical fine tuning of the position of the objective in the next months.
4. The lens in front of the camera has also a two-angle tilt mount.

With these elements we had enough to properly focus both the pump and the probe beams at the same point, since forming an image of the sample's surface on the camera ensures that the sample is on the focal plane of the microscope, although chromatic dispersion can make that either the probe or pump beams do not focus exactly on the same point. This can be corrected by some additional optics for future refinements, although we didn't find this point relevant in the current version of the experiment.

5.6. The synchronous detection

The pulsed laser of the setup has a repetition rate $\nu_L = 80\text{MHz}$, thus the time between two pulses is $T_L = 1/\nu_L = 12.5\text{ns}$. As explained before, the laser beam is divided into two beams, the pump and the probe, and the pump is modulated by the acousto-optic modulator with a square signal of frequency $\nu_M = 1.6\text{MHz}$, so that only $N = \nu_L/2\nu_M = 25$ pulses of the pump arrive to the samples each $T_M = 1/\nu_M$ seconds.

The effect of the pump on the sample is to change its reflectance during the transient effect of the excitation of the thermoelastic effect, thus we can assume that the time dependent reflectance $R(t)$ has a shorter duration than T_L (this might not be true for high repetition rates, but we will assume it for now), the reflectance of the sample will be therefore a periodic signal with period T_M such that

$$R_M(t) = \sum_{n=1}^N R(t - nT_L)$$

This reflectance is interrogated by the probe beam, which is a train of pulses at frequency ν_L , and delayed a time t_0 , which we can control with the delay line. Therefore, the intensity arriving to the balanced photodiode and then to the lock-in amplifier will be

$$I(t) = \sum_{n=1}^N I_0 (R(t - nT_L) - 1) \delta(t - t_0 - nT_L)$$

This function can be expressed as a Fourier series of fundamental frequency ν_M , thus we will have

$$I(t) = \sum_{\ell=1}^{\infty} I_{\ell} e^{i2\pi\ell\nu_M t}$$

since the term $\ell = 0$ is set to zero upon subtraction with the reflectance at rest. We have then

$$I_\ell = \frac{1}{T_M} \int_0^{T_M} dt \sum_{N=1}^N R(t - nT_L) e^{2i\pi\ell\nu_M t} = \sum_{n=1}^N \hat{I}_\ell e^{2i\pi\ell nT_L/T_M}$$

where we have defined

$$\hat{I}_\ell = \frac{1}{T_M} \int_0^{T_M} I_0 R(t) \delta(t - t_0) e^{2i\pi\ell t/T_M} dt = \frac{1}{T_M} I_0 R(t_0) e^{2i\pi\ell t_0/T_M}$$

The lock-in amplifier will be locked to the modulation frequency ν_M , thus we will be able to detect only the $\ell = 1$ term, which is

$$I_1 = \frac{N}{T_M} I_0 R(t_0) e^{2i\pi t_0/T_M}$$

since $T_M/T_L = N$ is an integer quantity.

Figure 7 shows a schematic view of the measurement process (not to scale). Panel a shows how the pump beam, made of a train of 400nm pulses, is modulated at a lower frequency by the AOM. In the figure we see only four pulses in the active period of the AOM but in practice we have 25. This pump makes that the reflectance of the sample be the one shown in panel b, which is a set of short-time pulses occurring only while the pump arrives. Panel c represents the train of pulses of the probe, with some (controllable) delay respect to the pump. As we see, the probe arrives during the full period of the AOM, consequently the reflected intensity will have the shape shown in panel d. Consequently, if the probe is capable of detect this variation in the reflectance its intensity will be modulated at the frequency of the AOM, which will be detected by the lock-in amplifier.

Whether if we are interested in the change of phase or in the change of modulus of the reflectance of the sample, the variations are extremely weak (of the order of 10^{-5}), and the most suitable method of detection of these variations is the synchronous detection. Then, the intensities of the two beams are measured by a balanced photodiode (Thorlabs PDB440A-AC) and their difference is sent to a lock-in amplifier (Stanford Instruments SR865A) in which the signal applied to the acousto-optic modulator is used as the reference signal. Any component at the modulation frequency in the lock-in will be due to the excitation of the surface by the pump.

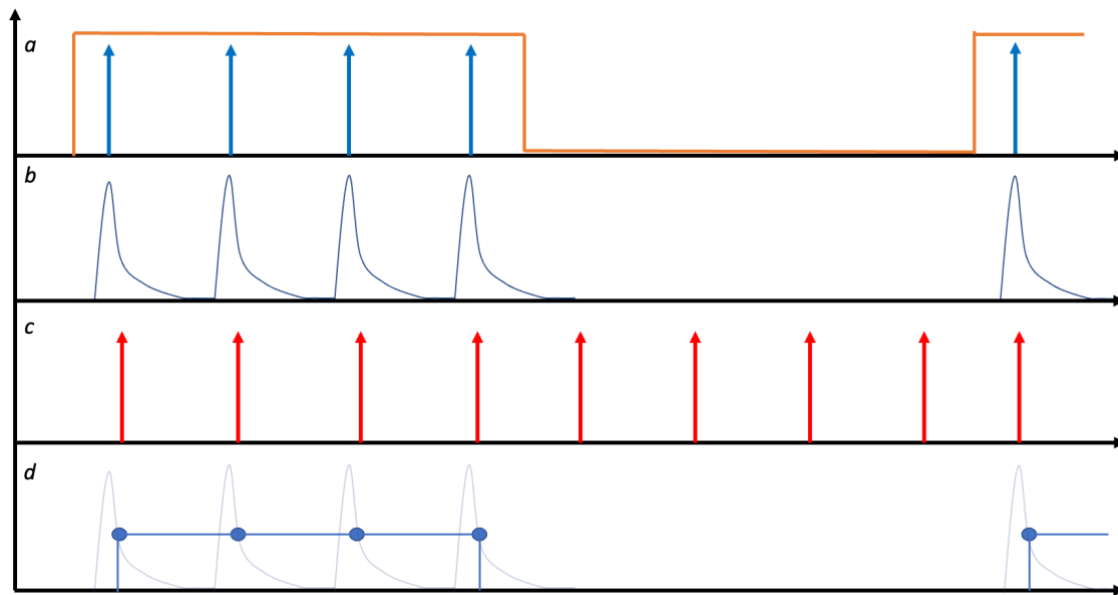


Figure 7 Time representation of the different processes taking place in the experiment (see text for a detailed explanation).

In our current setup we had to be very conservative in setting the parameters of the Lock-in amplifier and the speed at which the delay line changes its position for the temporal scan, thus we had to set the time constant of the lock-in to 300ms and the speed of the delay line to 0.1mm/s. Other parameters like input range and sensibility strongly depend on the specific signal to be measured, which may vary from one sample to another and are easily adjustable.

6. Future improvements

Although the preliminary results show that we have the correct fundamental configuration to properly excite and detect both bulk and surface acoustic waves, there is still room of improvement for the current setup. While the refinement of this kind of setup can last the full duration of the project, we have identified the following main issues for the next months:

1. Configuration of the Sagnac interferometer to make it phase sensitive. As mentioned before, the current version of the setup does not make use of the full interferometric features of the Sagnac-like interferometer, since the difference of signals in the photodiodes is proportional to the modulus of the reflectance only. The use of this interferometer requires a fine tuning of the polarization states of the beams, and for this purpose we might need to improve the quality of some polarizers of the setup and improve the alignment of the setup. This refinement will allow us to make measurements of SAWs with more precision.
2. Include a transverse scanning system for the probe beams. We aim to scan the surface of the samples to get space-time resolved acoustic fields, consequently this part of the setup will be the main improvement within the next few months. Given the expertise of the team at UJI, we will try to use SLM, although if these do not give us the desired resolution, we will implement a scanning system based on a galvanometric mirror.

3. Imaging system. We would like to improve the imaging of the sample on the microscopic camera, since it is imperative to know the relative position of the pump and probe beams to be sure that the excitation of the fields is the right one.
4. Independent focusing for the pump beam. Since the wavelengths of the pump and probe goes to the two extremes of the visible spectrum, the microscope objective presents chromatic dispersion, thus the pump (400nm) and the probe (800nm) do not focalize at the same distance. We will implement a telescopic system for the pump to correct this defocusing.
5. Include a SLM for the pump. The excitation of several modes for the use of the phononic architectures as imaging devices might require the use of structured light for the pump since the point-like excitation will not be enough for a broadband generation. We will use SLM to accomplish this objective.

7. Conclusion

In summary, the setup for developing applications of phononic architectures is functioning properly, although there is room for improvement. Nevertheless, we can now begin to compare the results obtained by CNRS with our own measurements. The setup requires careful alignment of the different laser beams that hit the samples, but we have observed good stability in this regard, indicating that the optomechanics we used in the setup are of the required quality. It is worth noting that some configurations of the setup may require high-quality polarizing elements, which we may need to refine in the future.

The electronic part of the measurement is the most critical point since we aim to detect very weak and noisy signals. However, we have excellent equipment and have configured it properly to ensure accurate measurements.

The upcoming experiments within the next few months will provide an excellent opportunity to test our setup's reliability and quality. These experiments will help us determine the setup's effectiveness in developing imaging applications, which is the most complex part of our project.